Annals of Nuclear Medicine Vol. 20, No. 4, 255–267, 2006

PET/CT today: System and its impact on cancer diagnosis

Eriko TSUKAMOTO and Shinji OCHI

Medical Cooperation Teishinkai Central CI clinic

Over the past six years, PET/CT has spread rapidly and replaced conventional PET. Although PET/CT is a combination of PET for functional information and CT for morphological information, their combination is synergistic. PET/CT fusion images result in higher diagnostic accuracy with fewer equivocal findings. This results in a greater impact on cancer diagnosis. With attenuation correction performed by the CT component, PET/CT can provide higher quality images over shorter examination times than conventional PET. As with all modalities, PET/CT has several characteristic artifacts such as misregistration due to respiration, overattenuation correction due to metals, etc. Awareness of these pitfalls will help the imaging physician use PET/CT effectively in daily practice.

Key words: positron-emission tomography; tomography scanners, X-ray computed; ^{18}F-FDG; radionuclide imaging

INTRODUCTION

ALTHOUGH we think of Positron Emission Tomography as a new modality of recent value in cancer diagnosis, the basic technique of PET is about 50 years old.[1] It was used primarily for academic investigations until the advent of ^{18}F-Fluorodeoxyglucose (FDG), which is taken up selectively by cancer cells.[2,3] Since cancer has become a leading cause of death all over the world, FDG-PET has gained popularity for its ability to diagnose cancer. Today, PET is not only a tool of academic investigations but also a tool of clinical practice. Over the past ten years, FDG-PET has been a focus of interest for clinical studies involving cancer diagnosis. Many papers about cancer diagnosis using FDG-PET have been published. It is now generally accepted that FDG-PET is useful for the evaluation of solitary pulmonary nodules,[4–6] staging of malignant lymphoma,[7–9] detection of local recurrence of colon cancer,[10–12] and many other indications.

With an increasing demand for a PET camera that is suitable for clinical practice, PET cameras have gone through several evolutions.[13] The progressively increasing speed of computers dramatically shortened the amount of time needed to process an image. New reconstruction algorithms resulted in image quality improvement. However, given the difficulties with anatomic resolution and the long duration of the transmission scan needed for attenuation correction, stand-alone PET still had serious limitations.

The advent of PET/CT solved these problems. A near-simultaneous acquisition of transmission and emission images, with diagnostic-quality CT images used for both attenuation correction and anatomic localization, PET/CT is more than its separate modalities.[14]

DEVELOPMENT OF PET/CT

Researchers realized early on that the morphologic information from CT and the functional information from PET would be ideal if they were combined.[15–17] Software registration techniques for the separate modalities provided more accurate localization than that provided by visual coregistration. However, several problems regarding erroneous registration resulted. Especially in the fusion of body images, deformable organs caused various errors. Time differences in imaging created other problems. For example, the contours of the abdomen are dependent on the pallet design; also, gastrointestinal organs move over time. This made accurate registration

Received May 8, 2006, revision accepted May 8, 2006.

For reprint contact: Eriko Tsukamoto, M.D., Medical Cooperation Teishinkai Central CI clinic, Sapporo Medi-Care center building, 1–27, Nishi 17, Odori, Chuo-ku, Sapporo 060–0042, JAPAN.

E-mail: tsukamoto@teishinkai.jp

Table 1 Main characters of the CT scanners integrated in the PET/CT system available in Japan

	GE Discovery ST Elite	Siemens Biograph	Toshiba Aquiduo16	Philips Gemini GXL	Shimadzu Eminence SOPHIA SET-3000GCT
Number of detector per row	8, 16	6, 16	16	6, 10, 16	1
360° full scan time (sec/rot)	0.5	0.5	0.5	0.5	0.75 (option 0.4)
Maximum scan field of view	50 (CTAC70)	50	50	50	50
Tube voltage (kvp)	80–140	80–140	80–135	90–140	80–135
Tube current (mA)	10–440	28–500	10–500	20–500	10–300
Heat capacity (HU)	6.3 M	5.3 M	7.5 M	8.0 M	4.5 M
Slice width	0.625, 1.25, 2.5, 3.75, 5, 7.5, 10	0.6–10	0.5, 1, 2, 3, 4, 6, 8	0.6–12	1, 2, 3, 5, 7, 10
Auto exposure control	yes	yes	yes	yes	no

Table 2 Main characters of PET scanners integrated in the PET/CT system available in Japan

	GE Discovery ST Elite	Siemens Biograph	Toshiba Aquiduo16	Philips Gemini GXL	Shimadzu Eminence SOPHIA SET-3000GCT
Acquisition mode	3D & 2D	3D	3D	3D	3D
Scintillator	BGO	LSO	LSO	GSO	GSO
Detector size (mm)	4.75 × 6.2 × 30	4.2 × 4.2 × 20	4 × 4 × 20	4 × 6 × 20	2.45 × 5.1 × 30
Number of detectors	13,440	24,336	24,336	17,864	39,600
Trans FOV (cm)	70	58.5	58.5	57	60
Axial FOV (cm)	15.7	16.2	16.2	18	26 (20.8, 15.6)
Max length of scan (cm)	160	180	180	190	180
Number of slices	47	81	81	Brain 90, WH 45	99
Slice pitch (mm)	3.27	2	2	Brain 2, WH 4	2.6
Trans resolution (center, mm)	5.1	4.2	4.2	4.1	3.5
Axial resolution (center, mm)	4.8	4.5	4.5	4.5	4.2
Sensitivity (cps/kBq)	2.0 (2D), 8.5 (3D)	5.7	4.8	8	19
Scatter fraction (%)	19 (2D), 36 (3D)	19	36	35	50
NECR (kcps·kBq/m*l*)	80 kcps·12 kBq/m*l*	93 kcps·29 kBq/m*l*	85 cps·24 kBq/m*l*	70 kcps·11 kBq/m*l*	60 kcps·9.8 Bq/m*l*
Reconstruction	2D VUE Point, 2D FBP, 2D OSEM, 3D VUE Point, 3D Rp, 3D FORE-IR	OSEM, DIFT, FBP	FBP, OSEM	3D-RAMLA, 3D-LOR	FBP, OSEM, DRAMA
Matrix size	64, 128, 256	128, 256, 512	128, 144, 256, 288	128, 256	
Reconstruction time (/frame)	Less than 2 minutes	1 minute	2 minutes	Less than 1 minute	1–5 minutes
Attenuation correction	X ray	X ray	X ray	X ray	^{137}Cs

extremely difficult.

PET/CT was designed to provide the solution to these shortcomings. The first PET/CT prototype was introduced by David Townsend and colleagues at University of Pittsburgh in 1998.[18,19] In this prototype, PET detector electronics were mounted to the rear portion of a CT gantry. The detectors consisted of 2 arrays of bismuth germinate (BGO) blocks covering an axial field of 16 cm with 24 partial rings of detectors, providing full 3D data. The CT and PET cameras were placed close together in the same gantry housing, with different consoles controlling the operation of the CT and the PET. In spite of separate operation, accurate image fusion and attenuation correction with CT data were possible with the two systems intrinsically aligned on the same mechanical support.

Hundreds of patients were imaged in clinical trials using this prototype PET/CT.[20–23] These clinical trials revealed the superiority of PET/CT image over either modality alone.

Encouraged by these data, various manufacturers made PET/CT scanners commercially available in Europe and the United States in 2001.

PET/CT scanner design

The first PET/CT system approved by FDA was marketed by Sidemen's (Siemens Medical Solutions, Erlangen, Germany) as the Biograph.[24] It incorporated a high-performance CT, a dual slice Somatom Emotion, and PET with fixed complete rings. CT and PET were placed tandem within the gantry housing. Instead of the old PET transmission sources, CT-based attenuation correction was standard on this system. The couch was changed so that vertical deflection of the pallet was eliminated.

At present, several vendors are producing PET/CT systems. Their PET/CT designs are basically the same.[25] PET/CT scanners consist of three main components: 1) a PET scanner, 2) a CT scanner, 3) a patient bed (Fig. 1). Currently, each PET/CT system consists of its latest high performance PET scanner and high performance multi-detector 2-16-slice CT. In addition to the older NaI and BGO scintillators, lutetium oxyorthosilicate (LSO), and gadolinium oxyorthosilicate (GSO) are available now and are used in the bulk of new installations. Acquisition mode is usually in 3D; only General Electric Medical Systems provide operation in 2D. Most of the PET/CT systems have a patient port with a larger diameter than stand-alone PET systems to match the CT port. Each vendor developed unique patient handling systems to reduce vertical deflection of the bed so that serious misalignment between PET and CT images would not occur. A single bed moves axially into the scanner and usually the patient undergoes the CT scan and then the PET scan. Characteristics of major PET/CT systems available in Japan are shown in the next section.

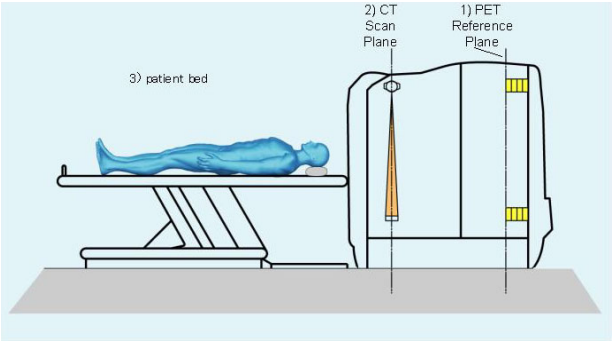

Fig. 1 Basic PET/CT scanner design.

PET/CT in Japan

Although PET/CT has spread rapidly in Europe and the United States, approval of the PET/CT scanner took a while in Japan. The first PET/CT approved in Japan was the Discovery LS manufactured by General Electric (GE Medical Systems, Milwaukee, Wisconsin, USA) in December 2003 followed by the Discovery ST in July 2004. Since then, several PET/CT cameras produced by other vendors have become available. Those cameras have different characteristics as shown in Tables 1 and 2. All the CT scanners have multiple detectors, up to 16. Each PET camera has its own unique characteristics in terms of scintillator materials, detector concepts, and reconstruction algorithms. At present, the PET/CT systems of five vendors are commercially available. Figure 2 shows their latest cameras.

Now, as in other countries, new cameras purchased in Japan are mostly PET/CT. Although there is no official data about PET/CT systems sold in Japan, the number could reach more than 150 by the end of 2006.

TECHNICAL CONSIDERATIONS

Image Fusion

Although PET and CT detectors are placed within the same gantry housing in PET/CT, its image fusion is not a

Fig. 2 Recent PET/CT systems commercially available in Japan.

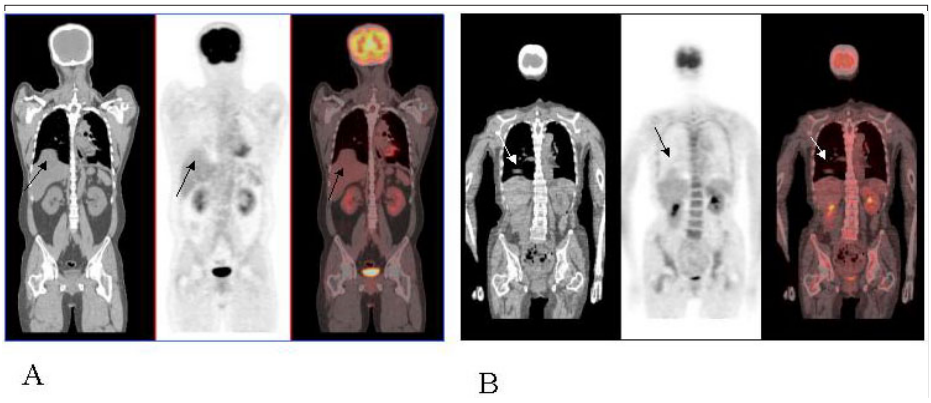

Fig. 3 Registration errors due to respiratory motion. A: Deformity of dome of the liver is noted (*arrows*). B: Separated liver dome activity is noted in the lung (*arrows*).

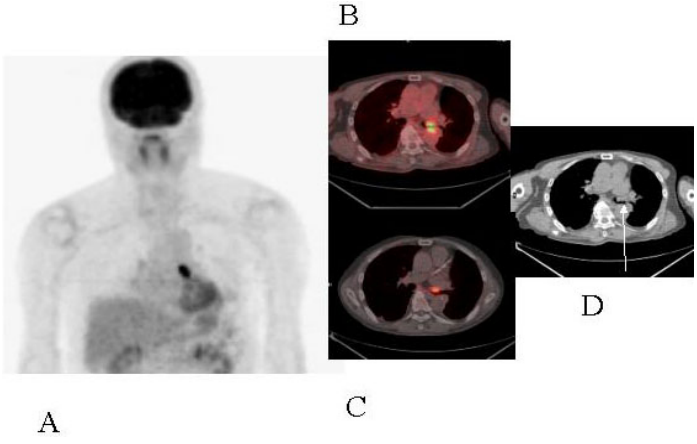

Fig. 4 Recurrence of tumor within left mainstem bronchus detected by FDG-PET. A: PET MIP image of the chest. B: Accumulation in the bronchus is noted on image taken with tidal breathing. C: With 30 second breathhold, accumulation of FDG is noted in tumor in the bronchus. D: CT image shows tumor inside of the bronchus (*arrow*).

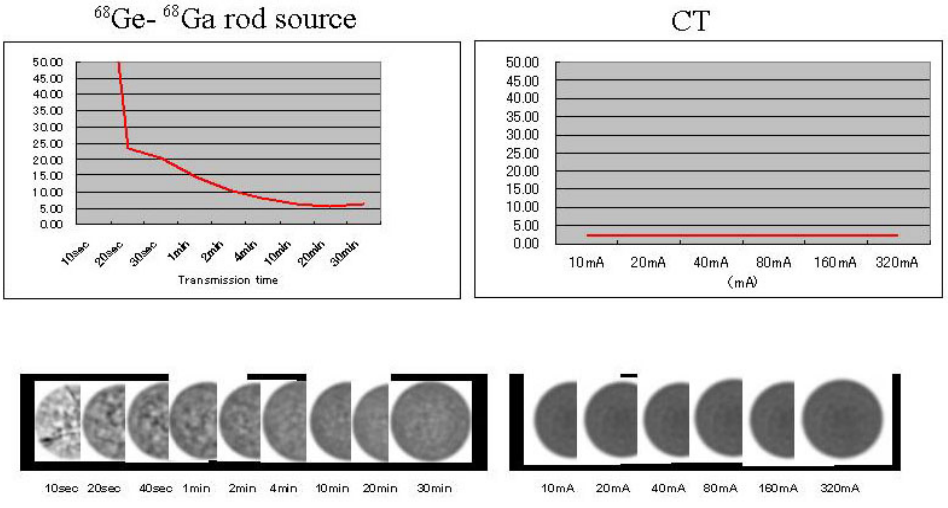

Fig. 5 Phantom attenuation images with CT and ^{137}Cs sources under various conditions. Graphs show relationship between coefficient of variation of the counts in the region of interest and transmission time with ^{68}Ge-^{68}Ga rod source or CT tube current. CT provides the same quality of transmission images even with the lowest tube current.

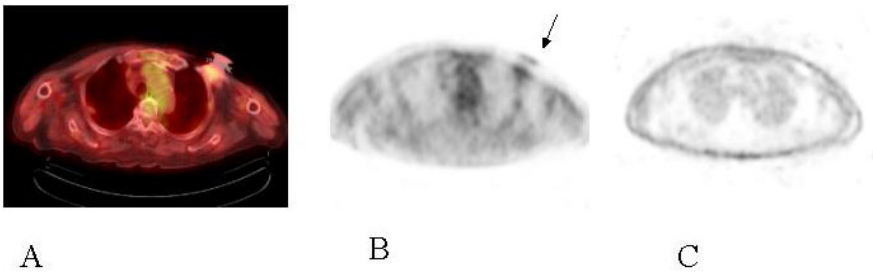

Fig. 6 Overcorrection of attenuation by pacemaker. A: a fusion image, B: image with attenuation correction, C: image without attenuation correction.

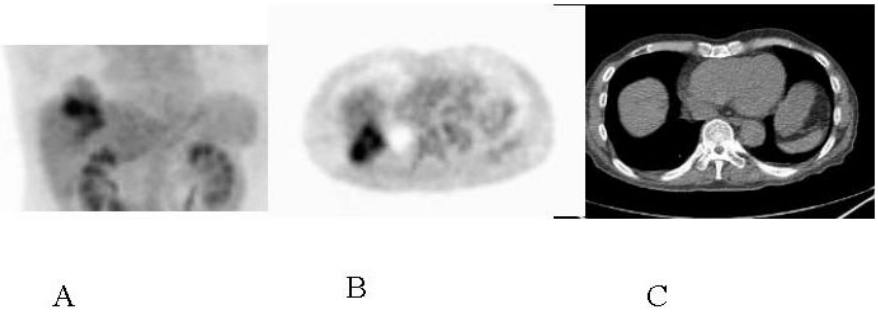

Fig. 7 Attenuation error in a liver lesion. A: PET MIP image of at the level of diaphragm, B: transaxial image of PET, C: CT image of same level of PET. No lesion is noted.

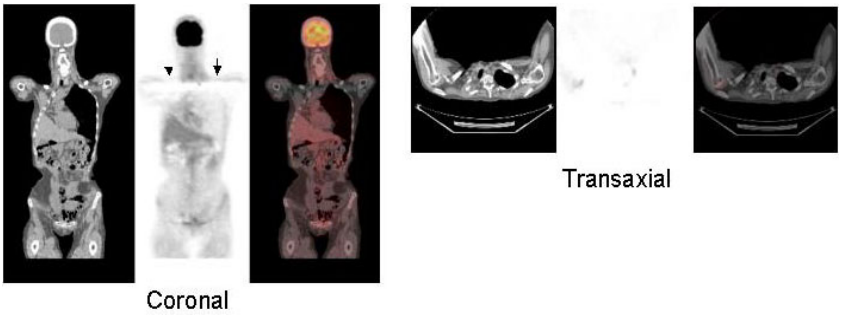

Fig. 8 Truncation error from arms. Photon deficient area is noted (*arrowheads*) at the level of the elbows, which are positioned outside of CT FOV.

true hardware fusion. They are operated separately and images taken by each camera are fused with software. They are, however, acquired with the same mechanical support and with the separate scanners positioned in-line at a fixed distance, which makes image fusion much more accurate than previous software fusion with images taken by separate camera systems at different times.[26,27] PET/CT solves the problem caused by body contour deformability and time difference, but does not routinely correct for breathing artifacts or inadvertent positioning changes between the two scans. CT scans are usually acquired during a breath hold while PET scans are acquired during free tidal breathing because of the long duration of scan. This difference in breathing techniques can cause misregistration (Fig. 3), especially in the organs most affected by respiratory motion. One of the available solutions is acquisition of CT scan during shallow breathing.[28,29] The other option is CT scanning during breath hold in a fixed position and best match with PET scan in unforced expiration,[30,31] which is not very easy to do for most patients. The ideal solution may be acquisition with respiratory gating, which is not widely used currently. Gated acquisition is, however, going to be a standard in the future and many systems for it are now being developed.[32–35] In our clinic, we are performing the PET scan with a 30-second inspiratory breath hold per bed position when misregistration is observed. Figure 4 is a patient with suspected lung cancer recurrence. FDG was taken up in the left mediastinum but it was difficult to localize the lesion on CT. With the 30 second breath hold, we can

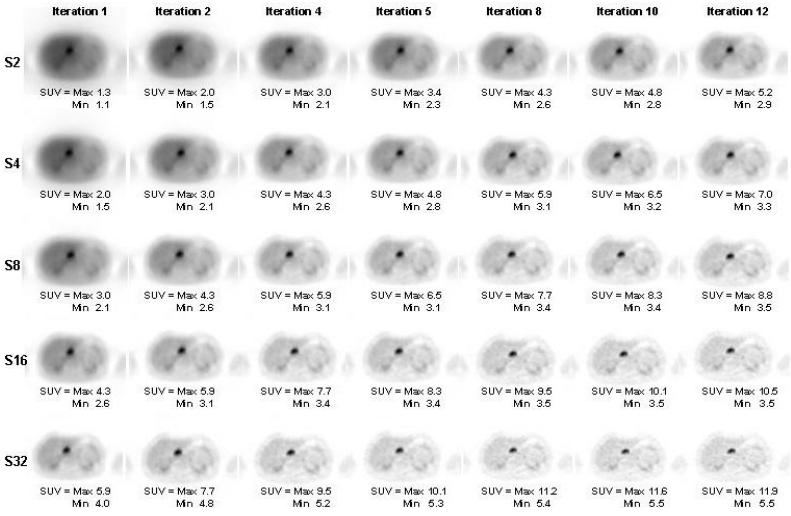

Fig. 9 Images reconstructed using OSEM. Subset and iteration numbers affect image quality and SUV.

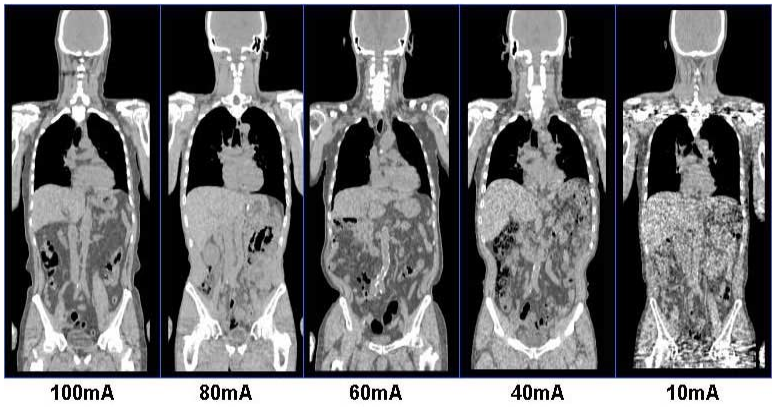

Fig. 10 CT images acquired with various tube currents.

clearly recognize the intense accumulation of FDG in the tumor inside of the left mainstem bronchus.

Arm position is another very important factor for image quality; sometimes patients move their arms because it is very tiring to keep the arms up for long time. Patients also move their heads, especially when they fall asleep during the examination. It is very important to use comfortable arm rests and to try to keep the patient awake during the examination.

CT-based attenuation correction

In the stand-alone PET systems, the effect of attenuation is corrected using external sources. Conventional PET uses either ^{68}Ge-^{68}Ga rod sources for 511-keV annihilation photons or ^{137}Cs point sources of 662-keV single-photon gamma rays for acquiring the transmission scan. This conventional method of transmission scanning needs significant time to collect sufficient photons; a transmission image obtained this way usually contains high levels of noise. A CT scan, on the contrary, needs a short time to scan the whole body and can provide a comparatively noiseless transmission image.[36,37] The multi-detector CT's which are used in current PET/CT models take less than 1 minute to scan whole body. It would take 60 minutes per bed position with ^{68}Ge-^{68}Ga rod sources to obtain a transmission image of CT quality. High-quality attenuation correction images are easily achievable with a low-dose CT scan.[38] Figure 5 shows phantom transmission images of CT and ^{137}Cs sources under various parameters.

CT attenuation values at a given energy depend on both the density and the relative element composition of the tissue. Attenuation coefficients are energy-dependent. Therefore the attenuation coefficients obtained by original CT images acquired at an energy of 60–80 keV needs to be scaled to those of 511 keV pixel by pixel.[18,39]

CT attenuation correction also has several disadvantages. One of them is overestimation of 511 keV attenuation values. It is usually associated with iodine- or barium-based contrast agents and metallic implants such as pacemakers, chemotherapy ports, dental fillings, ortho-

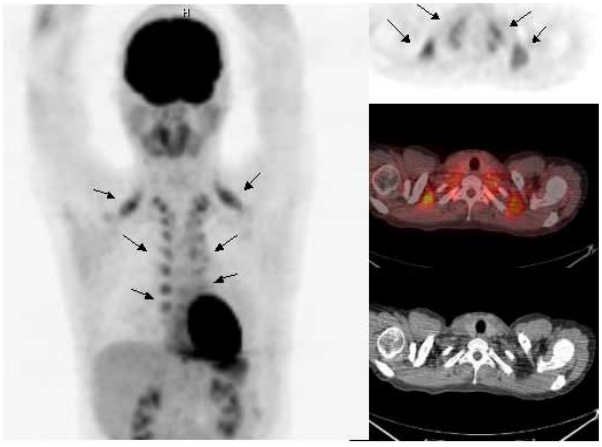

A B

Fig. 11 Typical example of brown fat. A: Symmetrical uptake is noted in supraclavicular area and the vicinity of spines. B: Transaxial images of PET, fusion and CT show uptake in the fat.

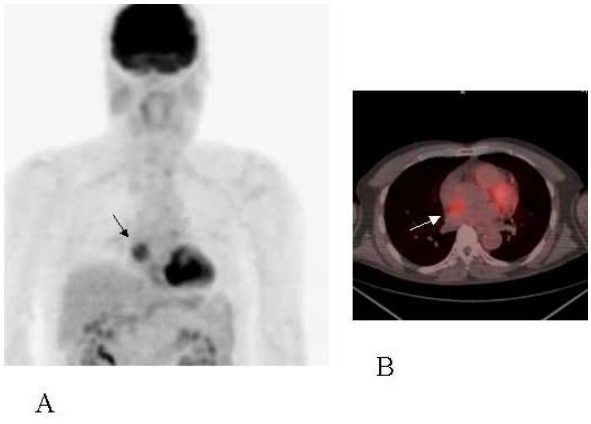

A B

Fig. 12 Mediastinal brown fat. A: PET MIP image chest shows uptake in the right mediastinum (*arrow*). B: Fusion image reveals uptake in the fat between right and left atrium (*arrow*).

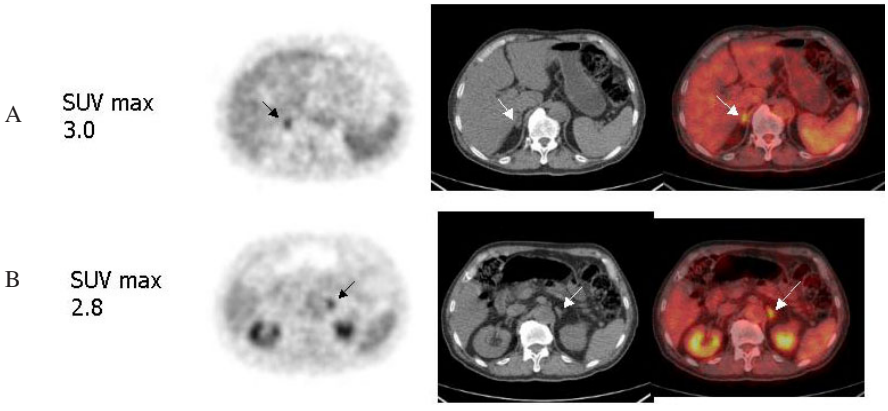

Fig. 13 Fusion images show FDG uptake in normal adrenal glands. A: FDG uptake in normal right adrenal gland. B: FDG uptake in normal left adrenal gland.

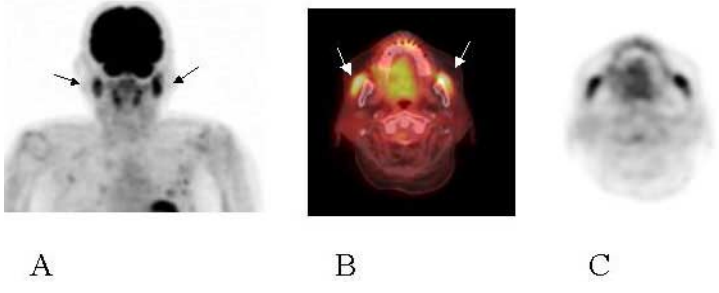

A B C

Fig. 14 Symmetrical facial muscle uptake (*arrows*). A: PET MIP image of face. B: Transaxial fusion image. C: Transaxial PET image.

pedic metal implants, etc.[40–43] As described earlier, the attenuation coefficients measured by CT scanning at an energy from 60–80 keV need to be scaled to those expected at 511 keV pixel by pixel. Most metals and contrast agents exhibit strong photoelectric absorption of X-rays but, like bone and other tissues, interact with 511-keV gammas primarily via Compton scattering. The CT-AC scaling algorithm does not account for this effect and causes overcorrection of PET images.[44,45] To avoid misinterpretation of the images, it is necessary to reconstruct

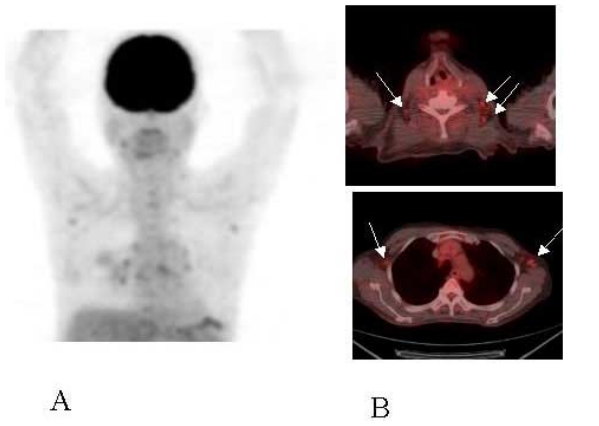

Fig. 15 A patient with follicular lymphoma. A: PET MIP image of head, neck, and chest. B: Fusion images show faint uptake in small lymph nodes (*arrows*).

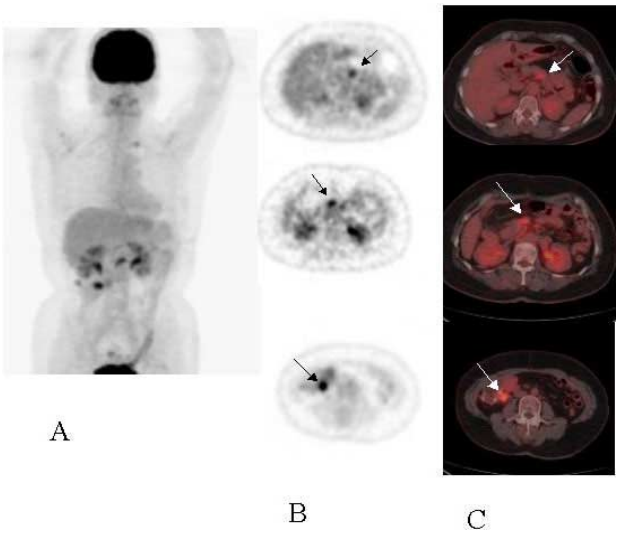

Fig. 16 Ovarian cancer patient with carcinomatous peritonitis A: Whole body PET MIP image. B: PET transaxial images. C: Transaxial fusion images clearly show metastatic nodules in peritoneal space.

PET images without attenuation correction when focal uptake might occur near structures with high CT numbers. Recently, several camera systems have methods such as the tissue conversion table used in the GE Discovery ST PET Scanner to reduce this artifact. Figure 6 shows overcorrection caused by a pacemaker.

The mismatch of PET and CT images due to patient respiration can have a marked effect on CT-derived attenuation correction as well as on image fusion.[46,47] The anatomic regions most affected by breathing artifacts include the diaphragm, lung bases, and liver dome. Figure 7 shows typical misregistration artifact at the level of the diaphragm. The possible solutions for this artifact have been described earlier.

Truncation error also causes an artifact.[48–50] In some cases, the arms may extend outside the transverse FOV of the CT scanner. Because the transverse FOV of the PET scanner is usually larger than that of the CT scanner, this results in missing data for the CT-based attenuation correction. This discrepancy in imaging FOV results in artifacts on the PET images (Fig. 8). Most of the recent PET/CT systems have algorithms for extrapolating the inconsistent CT projections to mitigate the truncation errors within the FOV of the CT scanner, and reduce the bias in the attenuation-corrected PET images.

OPTIMAL PROTOCOL

Patient preparation

The patient preparation for PET/CT is the same as that for conventional PET. Patients are fasted at least 4 hours prior to the injection of FDG. Diabetic patients should be in a stable state of disease management. Insulin levels greatly affect the biodistribution of FDG.[51] Therefore, insulin should not be administered before PET scan to lower the blood sugar. When control of blood sugar is difficult, examination is better performed in the patient with hyperglycemia. In that situation, accumulation of FDG is usually diffusely low. Patients are requested to drink water for hydration prior to the study in some PET centers.

Patient positioning

Prior to the examination, all metal such as dental braces, belt buckles, clothes with zippers and so on should be removed to avoid artifacts on both CT and PET scan. After bladder emptying to reduce radioactivity in the bladder, the patients are positioned supine on the bed with either arms up or down. They are usually positioned with the arms raised over the head to avoid CT beam hardening artifact. Additionally, because recent CT systems have automatic exposure control, the radiation dose increases in patients with their arms at their sides. As it usually takes around 30 minutes to complete the scan, comfortable arm rests are needed to reduce patient discomfort.[52] In contrast, the arms should be placed along the body in patients with head and neck tumors. Other devices such as comfortable pillows, foam pallets or vacuum bags for immobilization of the patients are also preferable for accurate fusion of images.

PET Protocol

PET protocol for PET/CT is basically the same as that for stand-alone PET. With the increased sensitivity of the latest PET cameras, the administered dose is getting lower and the acquisition time is getting shorter. It is, however, important to validate the optimal dose and acquisition time in each PET center.[53] Especially in obese patients, longer acquisition time is necessary to acquire an image of comparable quality.[54,55] Often, PET imaging extends from the base of the skull to the pubic symphysis. It is, however, important to cover all the extremities in patients

with malignant melanoma and in any other cases where involvement of the extremities is expected. Careful evaluation of the patients' history is always necessary.

In most PET cameras, an iterative attenuation-weighed ordered-subset expectation maximization algorithm (OSEM), using CT-based attenuation and scatter correction, is employed for the reconstruction of PET data. The optimal number of iterations and subsets is usually proposed by camera vendors and so are the filters. However, they should be evaluated by each PET center to confirm if they are optimal for that center's patient population. These parameters of PET/CT differ from those of conventional PET. They also influence standard uptake values (SUV) (Fig. 9).[56]

CT Protocol

Whole-body PET/CT examinations involve more radiation exposure to the patient than conventional PET examinations. Therefore, the added CT protocol for PET/CT must be justified in each case to avoid overexposure of patients to radiation for image quality that may not be needed.[57–60] Figure 10 shows CT images with varying tube currents, resulting in different levels of exposure.

In practice, for the CT protocol, one of two options may be chosen. One is CT as part of the PET/CT, used as a fast transmission measurement for attenuation correction and for anatomic labeling of the PET findings. In this case, the patient will have previously undergone a complete CT examination. Therefore, the radiation dose should be limited to reduce radiation exposure to the patient even though CT image quality will be suboptimal. The other is state-of-the-art CT, where diagnostic CT is clinically indicated. In this case, the examination should be performed with adequate radiation dose, and with contrast agent when necessary. When contrast agent is administered, timing of the CT scan will be determined depending on the body parts to be explored and the underlying disease being investigated.[61–63] Effect of contrast agent on attenuation correction also should be kept in mind.[64–66]

In Japan, because reimbursement of CT as a part of PET/CT had not been determined, CT was not performed as a diagnostic exam. However, reimbursement of PET/CT has been approved in April 2006 in Japan, and the CT protocol in PET/CT in Japan will be adjusted accordingly.

IMAGE INTERPRETATION AND CLINICAL SIGNIFICANCE

Physiologic accumulation

Image interpretation of PET/CT is not very different from that of conventional PET. Nonphysiologic uptake is recognized as abnormal. Compared with conventional PET, it is easier to distinguish physiological foci from abnormal foci with PET/CT. PET/CT has been shown to reduce the false-positive interpretation of physiological uptake.[67,68]

One of the confusing examples of physiological uptake, which is correctly recognized by PET/CT but not by PET, is brown fat.[69–71] There are two types of adipose tissue: white fat that stores energy and brown fat, which plays an important role in cold-induced and diet-induced thermogenesis. With stand-alone PET, increased symmetrical uptake in the neck had been interpreted as physiological uptake in muscle. However, fusion PET/CT images subsequently revealed that, in many cases, these accumulations were localized to brown adipose tissue. Cohade et al. first reported these accumulations as USA-FAT (Uptake in Supraclavicular Area) (Fig. 11).[72] Actually, brown fat exists in other locations as well, and it is often not symmetrical.[73,74] It is important not to confuse these physiologic accumulations with malignancy. A typical example is brown fat in the mediastinum, which was reported by Trung et al. (Fig. 12).[75]

The wide range of normal uptake in the adrenal glands is also clarified by PET/CT while it is difficult to recognize by conventional PET. Earlier papers on adrenal uptake by conventional PET described that most uptake in the adrenal gland was due to malignancy.[76–78] Now there is increasing awareness of the spectrum of normal adrenal uptake (Fig. 13)[79] as well as uptake in benign adrenal adenomas.[80]

Focal uptake in normal muscle (Fig. 14) and colon, often difficult with conventional PET, is also easy to recognize as physiological with PET/CT.

Impact on cancer diagnosis

Although PET/CT is a combination of PET and CT, its results are not additive but highly synergistic. Side-by-side analysis of CT and conventional PET is well-established. It is often difficult to achieve sufficient diagnostic clarity using conventional PET without the aid of CT.[81] Buell et al. reported that side-by-side reading is sufficient for diagnosis in most cases and PET/CT is needed in a few cases.[82] Antoch et al. concluded that tumor staging with PET/CT is significantly more accurate than CT alone, PET alone, and side-by-side reading of PET and CT.[83] Lardinois et al. analyzed the additional value of PET/CT in patients with non-small cell lung cancer.[84] PET/CT allowed for more exact localization of metastases and more precise determination of the local extent of primary tumor in about 40% of patients compared with conventional side-by-side reading of PET and CT. There are several discussions about this issue, but it is evident that it is much easier to reach an accurate diagnosis with PET/CT than with side-by-side reading of separately performed PET and CT examinations.

PET/CT has a slight advantage over side-by-side reading of PET and CT in characterization of known malignant lesions. Because the location of lesions is already known by other modalities, PET findings are the most important thing to be considered. A separate diagnostic CT scan can play an adequate role in precise diagnosis.

In restaging, localization of recurrence, and unknown primary tumors, PET/CT has a greater advantage over side-by-side reading of PET and CT.[85–88] It allows accurate and precise location of lesions. PET/CT increases reader confidence, reduces equivocal findings, and helps achieve an accurate diagnosis. PET/CT sometimes detects unsuspected foci which are difficult to identify on CT. Even with side-by-side reading it is often difficult to identify the anatomic area taking up the agent. Small lymph nodes are one example.[89] It is often important to identify their exact location, especially when biopsy of the lesion is necessary. Small lymph nodes are often difficult to identify with conventional PET because the uptake is usually very faint and difficult to distinguish from background, but it is not very difficult to localize even faint uptake in small lymph nodes by PET/CT by recognizing the uptake is superimposed on the visible lymph nodes. Especially in low-grade malignant lymphoma, thanks to PET/CT, we now can identify these small lymph node lesions with faint uptake, which is essential for staging (Fig. 15).[90,91]

The advantage of PET/CT over PET may be even greater in the abdomen than in the head, neck, and thorax. The peristalsis of the gastrointestinal tract and the variable filling states of hollow organs cause problems on side-by-side reading of PET and CT acquired at different times. Especially in the case of peritoneal spread, where lesions are often difficult to distinguish from normal gastrointestinal tract activity, PET/CT confers a large advantage (Fig. 16).[92–94]

Radiation therapy planning

PET/CT does not only improve diagnostic accuracy but has an impact on therapy planning by more exact and accurate location of the lesions. PET/CT may play an important role in radiation therapy planning. PET/CT imaging provides molecular information about a tumor in addition to morphological information to aid planning. Prior to using PET/CT in the radiation therapy planning process, the data transfer between the PET/CT system and the therapy planning system must be validated and quantitative accuracy of displayed values should be verified.[95] It is very important to put the patient in the position planned for later radiation therapy when PET/CT examination is performed. The same flat radiation pallet and fixation devices planned for radiation therapy are necessary for the PET/CT examination.[45] A preliminary report described that PET/CT significantly improves the measurement of gross tumor volume, one of the key volumes to be identified in radiation therapy planning.[96] Many centers of radiation oncology are already starting to use PET/CT for radiation therapy planning.[97–100] However, data regarding radiotherapy planning and PET/CT are still sparse and several issues remain to be solved before PET/CT is routinely used for radiotherapy planning.

CONCLUSION

In only 6 years, PET/CT systems have become widespread throughout the world. PET/CT has made it possible to acquire functional and anatomical data at the same time. It has improved PET interpretation dramatically, resulting in improved cancer diagnosis. PET/CT may become a major diagnostic tool for cancer diagnosis in the near future. PET/CT imaging is also potentially useful in radiation therapy planning, adding functional information to anatomical information.

There are still several problems to be solved in performing PET/CT. PET/CT has characteristic artifacts and other disadvantages different from those that arise with conventional PET. We must understand the unique characteristics of PET/CT and make an effort to use this revolutionary modality effectively.

REFERENCES

1. Frazee D. Positron emission tomography: a technology assessment of PET imaging—past, present, and future. *Radiol Manage* 2004; 26: 38–43.
2. Fukuda H, Matsuzawa T, Abe Y, Endo S, Yamada K, Kubota K, et al. Experimental study for cancer diagnosis with positron-labeled fluorinated glucose analogs: [^{18}F]-2-fluoro-2-deoxy-D-mannose: a new tracer for cancer detection. *Eur J Nucl Med* 1982; 7: 294–297.
3. Irie T, Ido T, Fukushi K, Iwata R, Uoji M, Tamate K, et al. Aspects of the preparation of ^{18}F-2-deoxy-2-fluoro-D-glucose (^{18}FDG) for medical use. *Radioisotopes* 1982; 31: 11–15.
4. Hubner KF, Buonocore E, Gould HR, Thie J, Smith GT, Stephens S, et al. Differentiating benign from malignant lung lesions using "quantitative" parameters of FDG PET images. *Clin Nucl Med* 1996; 21: 941–949.
5. Hagberg RC, Segall GM, Stark P, Burdon TA, Pompili MF. Characterization of pulmonary nodules and mediastinal staging of bronchogenic carcinoma with F-18 fluorodeoxyglucose positron emission tomography. *Eur J Cardiothorac Surg* 1997; 12: 92–97.
6. Bury T, Dowlati A, Paulus P, Corhay JL, Benoit T, Kayembe JM, et al. Evaluation of the solitary pulmonary nodule by positron emission tomography imaging. *Eur Respir J* 1996; 9: 410–414.
7. Kostakoglu L, Goldsmith SJ. Fluorine-18 fluorodeoxyglucose positron emission tomography in the staging and follow-up of lymphoma: is it time to shift gears? *Eur J Nucl Med* 2000; 27: 1564–1578.
8. Sasaki M, Kuwabara Y, Koga H, Nakagawa M, Chen T, Kaneko K, et al. Clinical impact of whole body FDG-PET on the staging and therapeutic decision making for malignant lymphoma. *Ann Nucl Med* 2002; 16: 337–345.
9. Yamamoto F, Tsukamoto E, Nakada K, Takei T, Zhao S, Asaka M, et al. ^{18}F-FDG PET is superior to ^{67}Ga SPECT in the staging of non-Hodgkin's lymphoma. *Ann Nucl Med* 2004; 18: 519–526.
10. Strauss LG, Clorius JH, Schlag P, Lehner B, Kimmig B, Engenhart R, et al. Recurrence of colorectal tumors: PET

evaluation. *Radiology* 1989; 170: 329–332.
11. Keogan MT, Lowe VJ, Baker ME, McDermott VG, Lyerly HK, Coleman RE. Local recurrence of rectal cancer: evaluation with F-18 fluorodeoxyglucose PET imaging. *Abdom Imaging* 1997; 22: 332–337.
12. Ogunbiyi OA, Flanagan FL, Dehdashti F, Siegel BA, Trask DD, Birnbaum EH, et al. Detection of recurrent and metastatic colorectal cancer: comparison of positron emission tomography and computed tomography. *Ann Surg Oncol* 1997; 4: 613–620.
13. Beyer T, Tellmann L, Nickel I, Pietrzyk U. On the use of positioning aids to reduce misregistration in the head and neck in whole-body PET/CT studies. *J Nucl Med* 2005; 46: 596–602.
14. von Schulthess GK. Positron emission tomography versus positron emission tomography/computed tomography: from "unclear" to "new-clear" medicine. *Mol Imaging Biol* 2004; 6: 183–187.
15. Alpert NM, Berdichevsky D, Levin Z, Morris ED, Fischman AJ. Improved methods for image registration. *Neuroimage* 1996; 3: 10–18.
16. Alyafei S, Inoue T, Zhang H, Ahmed K, Oriuchi N, Sato N, et al. Image Fusion System Using PACS for MRI, CT, and PET Images. *Clin Positron Imaging* 1999; 2: 137–143.
17. Barra V, Boire JV. A general framework for the fusion of anatomical and functional medical images. *Neuroimage* 2001; 13: 410–424.
18. Kinahan PE, Townsend DW, Beyer T, Sashin D. Attenuation correction for a combined 3D PET/CT scanner. *Med Phys* 1998; 25: 2046–2053.
19. Townsend DW, Carney JP, Yap JT, Hall NC. PET/CT today and tomorrow. *J Nucl Med* 2004; 45 Suppl 1: 4S–14S.
20. Beyer T, Townsend DW, Brun T, Kinahan PE, Charron M, Roddy R, et al. A combined PET/CT scanner for clinical oncology. *J Nucl Med* 2000; 41: 1369–1379.
21. Kluetz P, Villemagne VV, Meltzer C, Chander S, Martinelli M, Townsend D. 20. The Case for PET/CT. Experience at the University of Pittsburgh. *Clin Positron Imaging* 2000; 3: 174.
22. Kluetz PG, Meltzer CC, Villemagne VL, Kinahan PE, Chander S, Martinelli MA, et al. Combined PET/CT Imaging in Oncology. Impact on Patient Management. *Clin Positron Imaging* 2000; 3: 223–230.
23. Martinelli M, Townsend D, Meltzer C, Villemagne VV. 7. Survey of Results of Whole Body Imaging Using the PET/CT at the University of Pittsburgh Medical Center PET Facility. *Clin Positron Imaging* 2000; 3: 161.
24. Brambilla M, Secco C, Dominietto M, Matheoud R, Sacchetti G, Inglese E. Performance characteristics obtained for a new 3-dimensional lutetium oxyorthosilicate-based whole-body PET/CT scanner with the National Electrical Manufacturers Association NU 2-2001 standard. *J Nucl Med* 2005; 46: 2083–2091.
25. Townsend DW, Beyer T, Blodgett TM. PET/CT scanners: a hardware approach to image fusion. *Semin Nucl Med* 2003; 33: 193–204.
26. Townsend DW, Beyer T. A combined PET/CT scanner: the path to true image fusion. *Br J Radiol* 2002; 75 Spec No: S24–30.
27. Kim JH, Czernin J, Allen-Auerbach MS, Halpern BS, Fueger BJ, Hecht JR, et al. Comparison between ^{18}F-FDG PET, in-line PET/CT, and software fusion for restaging of recurrent colorectal cancer. *J Nucl Med* 2005; 46: 587–595.
28. Beyer T, Antoch G, Blodgett T, Freudenberg LF, Akhurst T, Mueller S. Dual-modality PET/CT imaging: the effect of respiratory motion on combined image quality in clinical oncology. *Eur J Nucl Med Mol Imaging* 2003; 30: 588–596.
29. Sarikaya I, Yeung HW, Erdi Y, Larson SM. Respiratory artefact causing malpositioning of liver dome lesion in right lower lung. *Clin Nucl Med* 2003; 28: 943–944.
30. Goerres GW, Burger C, Schwitter MR, Heidelberg TN, Seifert B, von Schulthess GK. PET/CT of the abdomen: optimizing the patient breathing pattern. *Eur Radiol* 2003; 13: 734–739.
31. de Juan R, Seifert B, Berthold T, von Schulthess GK, Goerres GW. Clinical evaluation of a breathing protocol for PET/CT. *Eur Radiol* 2004; 14: 1118–1123.
32. Nehmeh SA, Erdi YE, Pan T, Pevsner A, Rosenzweig KE, Yorke E, et al. Four-dimensional (4D) PET/CT imaging of the thorax. *Med Phys* 2004; 31: 3179–3186.
33. Ay MR, Zaidi H. Development and validation of MCNP4C-based Monte Carlo simulator for fan- and cone-beam x-ray CT. *Phys Med Biol* 2005; 50: 4863–4885.
34. Larson SM, Nehmeh SA, Erdi YE, Humm JL. PET/CT in non-small-cell lung cancer: value of respiratory-gated PET. *Chang Gung Med J* 2005; 28: 306–314.
35. Boucher L, Rodrigue S, Lecomte R, Benard F. Respiratory gating for 3-dimensional PET of the thorax: feasibility and initial results. *J Nucl Med* 2004; 45: 214–219.
36. Cohade C, Wahl RL. Applications of positron emission tomography/computed tomography image fusion in clinical positron emission tomography—clinical use, interpretation methods, diagnostic improvements. *Semin Nucl Med* 2003; 33: 228–237.
37. Seemann MD. PET/CT: fundamental principles. *Eur J Med Res* 2004; 9: 241–246.
38. Kamel E, Hany TF, Burger C, Treyer V, Lonn AH, von Schulthess GK, et al. CT vs ^{68}Ge attenuation correction in a combined PET/CT system: evaluation of the effect of lowering the CT tube current. *Eur J Nucl Med Mol Imaging* 2002; 29: 346–350.
39. Burger C, Goerres G, Schoenes S, Buck A, Lonn AH, Von Schulthess GK. PET attenuation coefficients from CT images: experimental evaluation of the transformation of CT into PET 511-keV attenuation coefficients. *Eur J Nucl Med Mol Imaging* 2002; 29: 922–927.
40. Goerres GW, Ziegler SI, Burger C, Berthold T, Von Schulthess GK, Buck A. Artifacts at PET and PET/CT caused by metallic hip prosthetic material. *Radiology* 2003; 226: 577–584.
41. Bujenovic S, Mannting F, Chakrabarti R, Ladnier D. Artifactual 2-deoxy-2-[$^{(18)}$F]fluoro-D-glucose localization surrounding metallic objects in a PET/CT scanner using CT-based attenuation correction. *Mol Imaging Biol* 2003; 5: 20–22.
42. Antoch G, Jentzen W, Freudenberg LS, Stattaus J, Mueller SP, Debatin JF, et al. Effect of oral contrast agents on computed tomography-based positron emission tomography attenuation correction in dual-modality positron emission tomography/computed tomography imaging. *Invest Radiol* 2003; 38: 784–789.
43. Antoch G, Freudenberg LS, Egelhof T, Stattaus J, Jentzen

W, Debatin JF, et al. Focal tracer uptake: a potential artifact in contrast-enhanced dual-modality PET/CT scans. *J Nucl Med* 2002; 43: 1339–1342.
44. DiFilippo FP, Brunken RC. Do implanted pacemaker leads and ICD leads cause metal-related artifact in cardiac PET/CT? *J Nucl Med* 2005; 46: 436–443.
45. Bockisch A, Beyer T, Antoch G, Freudenberg LS, Kuhl H, Debatin JF, et al. Positron emission tomography/computed tomography—imaging protocols, artifacts, and pitfalls. *Mol Imaging Biol* 2004; 6: 188–199.
46. Robinson P, Parkin A. Respiratory motion artefacts on PET/CT. *Eur J Nucl Med Mol Imaging* 2003; 30: 1712.
47. Papathanassiou D, Becker S, Amir R, Meneroux B, Liehn JC. Respiratory motion artefact in the liver dome on FDG PET/CT: comparison of attenuation correction with CT and a caesium external source. *Eur J Nucl Med Mol Imaging* 2005; 32: 1422–1428.
48. Sourbelle K, Kachelriess M, Kalender WA. Reconstruction from truncated projections in CT using adaptive detruncation. *Eur Radiol* 2005; 15: 1008–1014.
49. Mawlawi O, Erasmus JJ, Pan T, Cody DD, Campbell R, Lonn AH, et al. Truncation Artifact on PET/CT: Impact on Measurements of Activity Concentration and Assessment of a Correction Algorithm. *AJR Am J Roentgenol* 2006; 186: 1458–1467.
50. Beyer T, Bockisch A, Kuhl H, Martinez MJ. Whole-Body ^{18}F-FDG PET/CT in the Presence of Truncation Artifacts. *J Nucl Med* 2006; 47: 91–99.
51. Torizuka T, Fisher SJ, Brown RS, Wahl RL. Effect of insulin on uptake of FDG by experimental mammary carcinoma in diabetic rats. *Radiology* 1998; 208: 499–504.
52. Beyer T, Antoch G, Muller S, Egelhof T, Freudenberg LS, Debatin J, et al. Acquisition protocol considerations for combined PET/CT imaging. *J Nucl Med* 2004; 45 Suppl 1: 25S–35S.
53. Watson CC, Casey ME, Bendriem B, Carney JP, Townsend DW, Eberl S, et al. Optimizing injected dose in clinical PET by accurately modeling the counting-rate response functions specific to individual patient scans. *J Nucl Med* 2005; 46: 1825–1834.
54. Halpern BS, Dahlbom M, Quon A, Schiepers C, Waldherr C, Silverman DH, et al. Impact of patient weight and emission scan duration on PET/CT image quality and lesion detectability. *J Nucl Med* 2004; 45: 797–801.
55. Halpern BS, Dahlbom M, Auerbach MA, Schiepers C, Fueger BJ, Weber WA, et al. Optimizing imaging protocols for overweight and obese patients: a lutetium orthosilicate PET/CT study. *J Nucl Med* 2005; 46: 603–607.
56. Jaskowiak CJ, Bianco JA, Perlman SB, Fine JP. Influence of reconstruction iterations on ^{18}F-FDG PET/CT standardized uptake values. *J Nucl Med* 2005; 46: 424–428.
57. Wu TH, Chu TC, Huang YH, Chen LK, Mok SP, Lee JK, et al. A positron emission tomography/computed tomography (PET/CT) acquisition protocol for CT radiation dose optimization. *Nucl Med Commun* 2005; 26: 323–330.
58. Li T, Schreibmann E, Thorndyke B, Tillman G, Boyer A, Koong A, et al. Radiation dose reduction in four-dimensional computed tomography. *Med Phys* 2005; 32: 3650–3660.
59. Wu TH, Huang YH, Lee JJ, Wang SY, Wang SC, Su CT, et al. Radiation exposure during transmission measurements: comparison between CT- and germanium-based techniques with a current PET scanner. *Eur J Nucl Med Mol Imaging* 2004; 31: 38–43.
60. Brix G, Lechel U, Glatting G, Ziegler SI, Munzing W, Muller SP, et al. Radiation exposure of patients undergoing whole-body dual-modality ^{18}F-FDG PET/CT examinations. *J Nucl Med* 2005; 46: 608–613.
61. Antoch G, Freudenberg LS, Beyer T, Bockisch A, Debatin JF. To enhance or not to enhance? ^{18}F-FDG and CT contrast agents in dual-modality ^{18}F-FDG PET/CT. *J Nucl Med* 2004; 45 Suppl 1: 56S–65S.
62. Brechtel K, Klein M, Vogel M, Mueller M, Aschoff P, Beyer T, et al. Optimized contrast-enhanced CT protocols for diagnostic whole-body ^{18}F-FDG PET/CT: technical aspects of single-phase versus multiphase CT imaging. *J Nucl Med* 2006; 47: 470–476.
63. Strobel K, Thuerl CM, Hany TF. How much intravenous contrast is needed in FDG-PET/CT? *Nuklearmedizin* 2005; 44 Suppl 1: S32–37.
64. Berthelsen AK, Holm S, Loft A, Klausen TL, Andersen F, Hojgaard L. PET/CT with intravenous contrast can be used for PET attenuation correction in cancer patients. *Eur J Nucl Med Mol Imaging* 2005; 32: 1167–1175.
65. Nakamoto Y, Chin BB, Kraitchman DL, Lawler LP, Marshall LT, Wahl RL. Effects of nonionic intravenous contrast agents at PET/CT imaging: phantom and canine studies. *Radiology* 2003; 227: 817–824.
66. Yau YY, Chan WS, Tam YM, Vernon P, Wong S, Coel M, et al. Application of intravenous contrast in PET/CT: does it really introduce significant attenuation correction error? *J Nucl Med* 2005; 46: 283–291.
67. Rosenbaum SJ, Lind T, Antoch G, Bockisch A. False-Positive FDG PET Uptake—the Role of PET/CT. *Eur Radiol* 2006; 16: 1054–1065.
68. Kostakoglu L, Hardoff R, Mirtcheva R, Goldsmith SJ. PET-CT fusion imaging in differentiating physiologic from pathologic FDG uptake. *Radiographics* 2004; 24: 1411–1431.
69. Minotti AJ, Shah L, Keller K. Positron emission tomography/computed tomography fusion imaging in brown adipose tissue. *Clin Nucl Med* 2004; 29: 5–11.
70. Hany TF, Gharehpapagh E, Kamel EM, Buck A, Himms-Hagen J, von Schulthess GK. Brown adipose tissue: a factor to consider in symmetrical tracer uptake in the neck and upper chest region. *Eur J Nucl Med Mol Imaging* 2002; 29: 1393–1398.
71. Yeung HW, Grewal RK, Gonen M, Schoder H, Larson SM. Patterns of $^{(18)}$F-FDG uptake in adipose tissue and muscle: a potential source of false-positives for PET. *J Nucl Med* 2003; 44: 1789–1796.
72. Cohade C, Mourtzikos KA, Wahl RL. "USA-Fat": prevalence is related to ambient outdoor temperature-evaluation with ^{18}F-FDG PET/CT. *J Nucl Med* 2003; 44: 1267–1270.
73. Heiba SI, Bernik S, Raphael B, Sandella N, Cholewinski W, Klein P. The distinctive role of positron emission tomography/computed tomography in breast carcinoma with brown adipose tissue 2-fluoro-2-deoxy-D-glucose uptake. *Breast J* 2005; 11: 457–461.
74. Bar-Shalom R, Gaitini D, Keidar Z, Israel O. Non-malignant FDG uptake in infradiaphragmatic adipose tissue: a new site of physiological tracer biodistribution characterised

by PET/CT. *Eur J Nucl Med Mol Imaging* 2004; 31: 1105–1113.
75. Truong MT, Erasmus JJ, Munden RF, Marom EM, Sabloff BS, Gladish GW, et al. Focal FDG uptake in mediastinal brown fat mimicking malignancy: a potential pitfall resolved on PET/CT. *AJR Am J Roentgenol* 2004; 183: 1127–1132.
76. Boland GW, Goldberg MA, Lee MJ, Mayo-Smith WW, Dixon J, McNicholas MM, et al. Indeterminate adrenal mass in patients with cancer: evaluation at PET with 2-[F-18]-fluoro-2-deoxy-D-glucose. *Radiology* 1995; 194: 131–134.
77. Erasmus JJ, Patz EF Jr, McAdams HP, Murray JG, Herndon J, Coleman RE, et al. Evaluation of adrenal masses in patients with bronchogenic carcinoma using ^{18}F-fluorodeoxyglucose positron emission tomography. *AJR Am J Roentgenol* 1997; 168: 1357–1360.
78. Maurea S, Mainolfi C, Bazzicalupo L, Panico MR, Imparato C, Alfano B, et al. Imaging of adrenal tumors using FDG PET: comparison of benign and malignant lesions. *AJR Am J Roentgenol* 1999; 173: 25–29.
79. Bagheri B, Maurer AH, Cone L, Doss M, Adler L. Characterization of the normal adrenal gland with ^{18}F-FDG PET/CT. *J Nucl Med* 2004; 45: 1340–1343.
80. Blake MA, Slattery JM, Kalra MK, Halpern EF, Fischman AJ, Mueller PR, et al. Adrenal lesions: characterization with fused PET/CT image in patients with proved or suspected malignancy—initial experience. *Radiology* 2006; 238: 970–977.
81. Reinartz P, Wieres FJ, Schneider W, Schur A, Buell U. Side-by-side reading of PET and CT scans in oncology: which patients might profit from integrated PET/CT? *Eur J Nucl Med Mol Imaging* 2004; 31: 1456–1461.
82. Buell U, Wieres FJ, Schneider W, Reinartz P. ^{18}FDG-PET in 733 consecutive patients with or without side-by-side CT evaluation: analysis of 921 lesions. *Nuklearmedizin* 2004; 43: 210–216.
83. Antoch G, Saoudi N, Kuehl H, Dahmen G, Mueller SP, Beyer T, et al. Accuracy of whole-body dual-modality fluorine-18-2-fluoro-2-deoxy-D-glucose positron emission tomography and computed tomography (FDG-PET/CT) for tumor staging in solid tumors: comparison with CT and PET. *J Clin Oncol* 2004; 22: 4357–4368.
84. Lardinois D, Weder W, Hany TF, Kamel EM, Korom S, Seifert B, et al. Staging of non-small-cell lung cancer with integrated positron-emission tomography and computed tomography. *N Engl J Med* 2003; 348: 2500–2507.
85. Israel O, Mor M, Guralnik L, Hermoni N, Gaitini D, Bar-Shalom R, et al. Is ^{18}F-FDG PET/CT useful for imaging and management of patients with suspected occult recurrence of cancer? *J Nucl Med* 2004; 45: 2045–2051.
86. Barranger E, Kerrou K, Petegnief Y, David-Montefiore E, Cortez A, Darai E. Laparoscopic resection of occult metastasis using the combination of FDG-positron emission tomography/computed tomography image fusion with intraoperative probe guidance in a woman with recurrent ovarian cancer. *Gynecol Oncol* 2005; 96: 241–244.
87. Gutzeit A, Antoch G, Kuhl H, Egelhof T, Fischer M, Hauth E, et al. Unknown primary tumors: detection with dual-modality PET/CT—initial experience. *Radiology* 2005; 234: 227–234.
88. Pelosi E, Pennone M, Deandreis D, Douroukas A, Mancini M, Bisi G. Role of whole body positron emission tomography/computed tomography scan with ^{18}F-fluorodeoxyglucose in patients with biopsy proven tumor metastases from unknown primary site. *Q J Nucl Med Mol Imaging* 2006; 50: 15–22.
89. Metser U, Golan O, Levine CD, Even-Sapir E. Tumor lesion detection: when is integrated positron emission tomography/computed tomography more accurate than side-by-side interpretation of positron emission tomography and computed tomography? *J Comput Assist Tomogr* 2005; 29: 554–559.
90. Allen-Auerbach M, Quon A, Weber WA, Obrzut S, Crawford T, Silverman DH, et al. Comparison between 2-deoxy-2-[^{18}F]fluoro-D-glucose positron emission tomography and positron emission tomography/computed tomography hardware fusion for staging of patients with lymphoma. *Mol Imaging Biol* 2004; 6: 411–416.
91. Tatsumi M, Cohade C, Nakamoto Y, Fishman EK, Wahl RL. Direct comparison of FDG PET and CT findings in patients with lymphoma: initial experience. *Radiology* 2005; 237: 1038–1045.
92. Bristow RE. Combined PET/CT for detecting recurrent ovarian cancer limited to retroperitoneal lymph nodes: Response to a letter from Dr. Maurie Markman. *Gynecol Oncol* 2006.
93. Sironi S, Messa C, Mangili G, Zangheri B, Aletti G, Garavaglia E, et al. Integrated FDG PET/CT in patients with persistent ovarian cancer: correlation with histologic findings. *Radiology* 2004; 233: 433–440.
94. Zissin R, Metser U, Hain D, Even-Sapir E. Mesenteric panniculitis in oncologic patients: PET-CT findings. *Br J Radiol* 2006; 79: 37–43.
95. Ciernik IF, Huser M, Burger C, Davis JB, Szekely G. Automated functional image—guided radiation treatment planning for rectal cancer. *Int J Radiat Oncol Biol Phys* 2005; 62: 893–900.
96. Ciernik IF, Dizendorf E, Baumert BG, Reiner B, Burger C, Davis JB, et al. Radiation treatment planning with an integrated positron emission and computer tomography (PET/CT): a feasibility study. *Int J Radiat Oncol Biol Phys* 2003; 57: 853–863.
97. Ashamalla H, Rafla S, Parikh K, Mokhtar B, Goswami G, Kambam S, et al. The contribution of integrated PET/CT to the evolving definition of treatment volumes in radiation treatment planning in lung cancer. *Int J Radiat Oncol Biol Phys* 2005; 63: 1016–1023.
98. Frank SJ, Chao KS, Schwartz DL, Weber RS, Apisarnthanarax S, Macapinlac HA. Technology insight: PET and PET/CT in head and neck tumor staging and radiation therapy planning. *Nat Clin Pract Oncol* 2005; 2: 526–533.
99. Leong T, Everitt C, Yuen K, Condron S, Hui A, Ngan SY, et al. A prospective study to evaluate the impact of FDG-PET on CT-based radiotherapy treatment planning for oesophageal cancer. *Radiother Oncol* 2006; 78: 254–261.
100. Messa C, Ceresoli GL, Rizzo G, Artioli D, Cattaneo M, Castellone P, et al. Feasibility of [^{18}F]FDG-PET and coregistered CT on clinical target volume definition of advanced non-small cell lung cancer. *Q J Nucl Med Mol Imaging* 2005; 49: 259–266.